



Optimization of elaboration conditions of ceramic membranes from animal bone through Design of Experiment (DoE) approach

M. Addich^{1*}, N. El Baraka^{1**}, A. Lknifli², K. Abbiche¹, N. Saffaj³, K. Sbihi²,
A. Ait Taleb¹, A. El Hammadi¹

¹Laboratory of Biotechnology, Materials, and Environment, Research-Research team: Physicochemistry of Natural Environments, Materials, and Environment, Polydisciplinary Faculty of Taroudant, Ibn Zohr University, BP 271, Taroudant, Morocco.

²Laboratory of Biotechnology, Materials, and Environment. Physicochemistry of Natural Environments, Materials, and Environment Team, Faculty of Sciences, Ibn Zohr University, BP 8106, Cite Dakhla, Agadir,

³Laboratory of Biotechnology, Materials, and Environment. Physicochemistry of Natural Environments, Materials, and Environment Team, polydisciplinary Faculty of Ouarzazate, Ibn Zohr University, BP 638, Ouarzazate, Morocco.

*Corresponding author, Email address: mourad.addich@gmail.com

**Corresponding author, Email address: n.elbaraka@uiz.ac.ma

Received 06 Jan 2022,
Revised 10 Feb 2022,
Accepted 12 Feb 2022

Keywords

- ✓ Design of experiment
- ✓ Porosity,
- ✓ Granulometry,
- ✓ Starch content,
- ✓ Sintering temperature.

mourad.addich@gmail.com
Phone: +212 23758196;

Abstract

The porosity and mechanical resistance of a ceramic membrane elaborated from animal bone has been studied using a design of experiment (DoE). The effect of Sintering temperature, Particle size and Starch content of the ceramic support membrane elaboration were evaluated using a complete factorial design 2³. Response Surface Methodology was used for further optimization. The supports have been prepared from animal bone with a two fraction 100 and 125 μm and a starch to enhance the performance of the support. The supports sintered between 900 °C and 1300 °C. By using DoE, it was found that the sintering temperature and particle size are the main controlling factors of the physical properties of ceramic support membrane. The increase of Sintering temperature had a positive effect on Mechanical strength and positive effect on porosity, on other hand the increase of particle size had a negative on porosity. The optimal factors to elaborate the membrane support by using DoE include a sintering temperature of 1300°C and starch content of 10% predicting the porosity of 15.7% and Mechanical strength of 17 MPa.

1. Introduction

Due to their potential application in a wide range of industrial processes, membrane technologies have received an increasing interest. The use of ceramic membranes has many advantages such as high thermal and chemical stability [1,2], long lifetime, and physic-chemical inertia [1]. From a technical-economic point of view, new composite ceramic microfiltration (MF) and ultrafiltration (UF) membranes have been produced recently from abundant natural materials like clay [3,4] and phosphate [5] as well as from animal bones [6]. These inorganic membranes have the advantage that they can be applied in extremely aggressive environments due to their distinct advantages.

In water treatment applications, the use of ceramic membranes is associated with numerous advantages relative to polymer-based filtration systems. High-temperature stability, fouling resistance, and low maintenance requirements contribute to lower lifecycle costs in such systems. However, the

high production costs of most commercially available ceramic membranes, stemming from raw materials and processing, are uneconomical for such systems in most water treatment applications.

The main concept of research on ceramic support membrane is to pay attention to support membrane morphology (porosity, pore size, and surface texture) as well as thermal, mechanical, and chemical stability. However, some factors such as chemicals mineralogical, particle size, organic additives, and processing procedures such as shaping, drying, and sintering temperature influence the performance of wet ceramic support membranes.

Preparation conditions can determine the membrane structure and performance ultimately. Thus, the good performance of ceramic membrane can be obtained by manipulating preparation conditions. In the past, researchers used one-factor-at-a-time experimental method, which not only consumed more time and more cost but also neglected the effect of interaction between factors [7]. An experiment with a good design and suitable model not only provides more information but also makes it possible to achieve optimal experimental conditions, while, a chemical experiment with a failed design may provide very poor information even when one uses a very good data analysis method to extract the chemical information from it. Thus, an efficient design for a chemical experiment is very important for chemists.

Many researches [8-11] have been written about designs of experiment in chemometrics. Design of the experiment is used to obtain a response chemical process with desirable characteristics in an efficient way.

Experimentally, many trials are required for evaluating, the effect of these factors and their mutual interaction on ceramic properties. The Experimental Design is generally used for the reduction of the number of experiments and the determination of a response value for any chosen natural variables belonging to the investigated experiments domains.

The aim is to understand first the effect of the factors and their interactions, and then to model the relationship between response y and factors (x_1, x_2, \dots, x_n) with a minimum number of experiments. This requires an orderly and efficient mapping of the experimental domain. Experimental design, when well applied, is therefore cost-saving.

This work consists to investigate the properties of the elaboration of ceramic wet support membrane from animal bone and evaluate the effects of Particle Size, sintering temperature and Starch content on porosity and mechanical strength using DoE approach. The selected factors that may have a significant effect on the elaboration of membrane support will be studied for optimizing factor and modeling the system by a mathematical model.

2. Materials and Methods

2.1 Experimental process

The shaping of a non-plastic ceramic powder requires the introduction of various organic compounds, which will make it possible to obtain a plastic paste with well-defined characteristics in the presence of water.

The plasticizer and binder organic additives are necessary to prepare a paste with rheological properties allowing shaping by extrusion that is why we have to optimize the initial formulation. All these additives can be removed during the heat treatment of the extruded part, which makes this process very usable [6,12].

The mixture of animal bone powder (81.7 % w/w) and organic additives was obtained by the mixture of bone powder and starch (corn starch RG03408, Cerestar) as the main factor, with Methocel 4% w / w (The Dow Chemical Company), Amijel 4% w / w (Cplus 12072, Cerestar) and PEG 1500

0.3% w / w (Prolabo). The mixture is stirred at 250 rpm, for 30 min in order to obtain good homogeneity. Water (32% w / w powders) and Zusoplast 0.24% w / w (Zschimmer and Schwartz) were also added and put in place for 30 min.

The pastes were kept in a closed box for 2 days under high humidity to avoid premature drying and to ensure complete diffusion of the water and organic additives. Thereafter they were shaped by extrusion into a thin film that was segmented to format flat disk supports with a diameter of 4.9 cm. Later, they were dried at temperature 40 °C during 24h of the flat support after extrusion. Finally, the extruded pieces were sintered in the furnace at 900-1300°C. The process of ceramic preparation is described in **Fig. 1**.

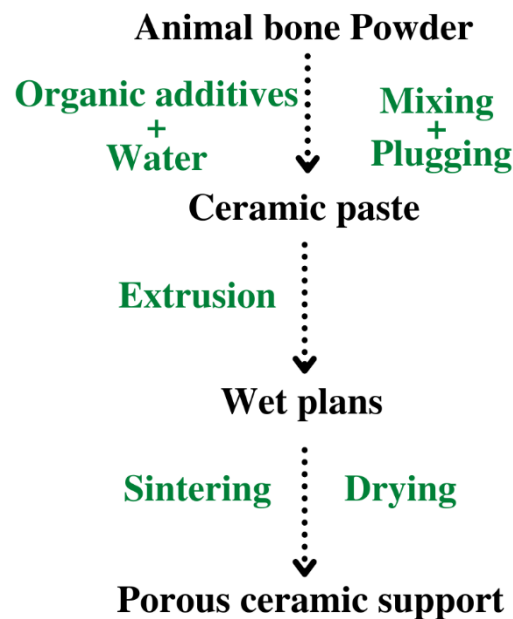


Figure 1: Diagram of porous support elaboration by extrusion method.

2.2 Mercury Porosimetry

The characterization of the quantity, size and size distribution of pores is an essential part of the investigation of refractories. Mercury intrusion porosimetry (MIP) is an analytical technique used to characterize the material's porous nature relating to the total pore volume, pore size distribution, bulk and apparent density which involves the intrusion of non-wetting mercury into the sample as a function of pressure [13].

The volume of intruded/extruded mercury is measured as a function of pressure and with the help of the Washburn equation based on the assumption of cylindrical pores. The imposed pressure p is converted into the corresponding pore radius r : $p = 2\gamma \cos \theta/r$, whereas θ is the contact angle and γ the surface tension of mercury [14].

Mercury porosimetry is an extremely useful characterization technique for porous materials. Pores between about 500 μm and 3.5 nm can be investigated [15]. One should keep in mind that the mercury intrusion porosimetry measures only open pores and solely the entryway between the surface of the sample and the pore cavities (largest entrance of a pore) and not the radius of the pore cavities itself [15].

This technique consists in gradually injecting mercury into a sample previously drained by increasing the pressure of the mercury. The relationship between the saturation of mercury and pressure can define the pressure curve which is linked to the structure of the pores. Porosity measurements by

mercury intrusion were performed by the AutoPore IV 9500 (MICROMERITICS) which allows to measure pore access diameters ranging from 0.003 to 1000 μm , for intrusion pressures between 0 and 200 MPa.

2.3 Design of experiment

There are different design of experiment methods including factorial designs, response surface designs, mixing designs and Taguchi designs (also called robust Taguchi designs). The design of experiment was applied to evaluate the effects of parameters and optimize conditions for various responses. BoxBehnken design of experiment (BBD) with three numeric factors on three different levels were used by Raj Mohan *et al.* [16].

The complete DoE approach adopted in our study involves three factors, such as particle Size (Granulometry)(X_1), the starch content (X_2) and sintering temperature (X_3), whose objective is to optimize the porosity (Y_1) and mechanical resistance (Y_2) considered as an answers, these factors which will be evaluated at two levels (a lower level marked -1 and a higher level marked +1) showed in **Table 1**.

Table 1: Factorial design of experiment 2^3 .

Level	Granulometry (μm)	Starch content (%)	Sintering temperature ($^{\circ}\text{C}$)
	X_1	X_2	X_3
-1	100	6	900
+1	125	10	1300

The design of experiments is a statistical method of multifactorial analysis of experimental data which provides a better understanding of the process than the standard methods of experimentation, since it is able to predict how the inputs affect the outputs in a complex process where different factors can interact among themselves. All the coefficients of the different polynomial equations [10,17]:

$$Y = a_0 + \sum_{i=1}^k a_i X_i + \sum_{i=1}^k \sum_{j=1}^k a_{ij} X_i X_j + \sum_i a_{ii} X_{ii}^2 + \varepsilon \quad \text{Eqn. 1}$$

Where Y is the response variable; a_0 is the intercept; a_i , a_{ij} and a_{ii} are coefficients of the linear effect, double interactions; X_i , X_j are the independent variables or factors and ε is error. An effective experiment design is therefore proposing to vary several factors both according to rules precise and rigorous organization: plans that we are going to study are multi factorials and usually called factorial designs. These "2 level and k factors 2^k " designs are the ones that should be used to research the factors acting on an answer measured. These are the simplest to interpret and they are the most cost-effective. Using a complete factorial design (**Fig.2**), we performed all the combinations of factor levels involved.

3. Results and Discussion

3.1 Experimental design and experimental results

The construction of a complete design is convenient to symbolize by -1 low level of each factor by +1 high level. Which allows you to collect the elements relating to each factor in a table called experience matrix, which is presented in correspondence with a column giving the experimental results of responses (Y_1 , Y_2). The following examples give the numerical values. The repeats to the eight experiments are indicated opposite, allowing the calculation of the effects (**Table 2**).

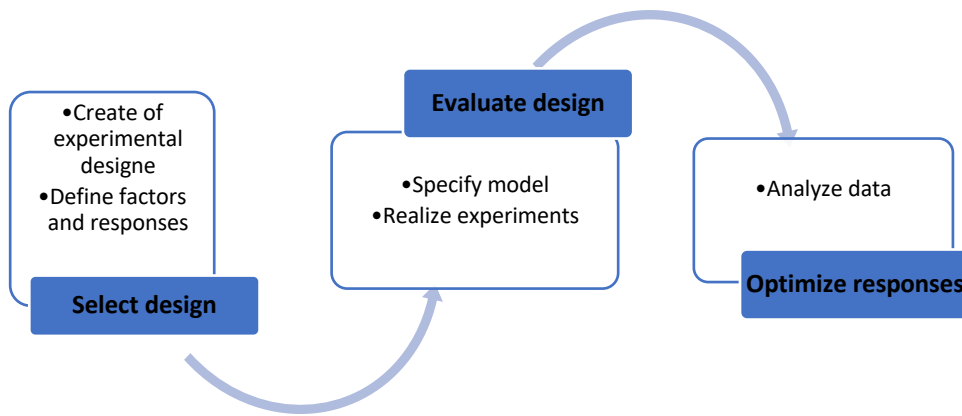


Figure 2: Schematization of a design of experiment.

Table 2: Design of experiment and Experimental Results

Experiments	Factors			Interactions				Responses	
	X_1	X_2	X_3	X_1X_2	X_1X_3	X_2X_3	$X_1X_2X_3$	Y_1 : Porosity (%)	Y_2 : Mechanical resistance (MPa)
1	-1	-1	-1	+1	+1	+1	-1	12.6	13.01
2	+1	-1	-1	-1	-1	+1	+1	10.3	13.03
3	-1	+1	-1	-1	+1	-1	+1	11.5	12.90
4	+1	+1	-1	+1	-1	-1	-1	10	13.03
5	-1	-1	+1	+1	-1	-1	+1	14.2	17.0
6	+1	-1	+1	-1	+1	-1	-1	14.0	17.04
7	-1	+1	+1	-1	-1	+1	-1	14.9	16.89
8	+1	+1	+1	+1	+1	+1	+1	15.7	16.9

3.2 Pareto diagram

The diagram of contribution illustrates the significance of the operating parameters. The negative or positive impact of the variables (sintering temperature, starch content and granulometry) on the output (porosity and mechanical resistance). **Figures 3** and **4** below show Pareto Diagram of the porosity and mechanical resistance of ceramic paste. From the diagram, we observe that the temperature has the highest positive effect on the porosity of the past followed by the granulometry of powder.

In this diagram, the effect of sintering temperature, interaction X_1X_3 , interaction X_2X_3 , and granulometry is important and contributes to maximize the response variations. On the other hand, the starch content does not have a significant effect. So, it is necessary to verify if this factor was not involved in the effect of the response to remove it in the analysis of variance. The powder granulometry is an important parameter because pore sizes and porosity of membranes are dependent on particles diameter.

The average effect of a factor is defined from the observed or modeled difference of response variable, when this factor undergoes a modality change. The scorecard and the average effect plot facilitate estimation and visualization of average effects. The effects plot of the medium facilitates the return of the information. This is an undeniable asset of the methodological approach associated with the design of experiments.

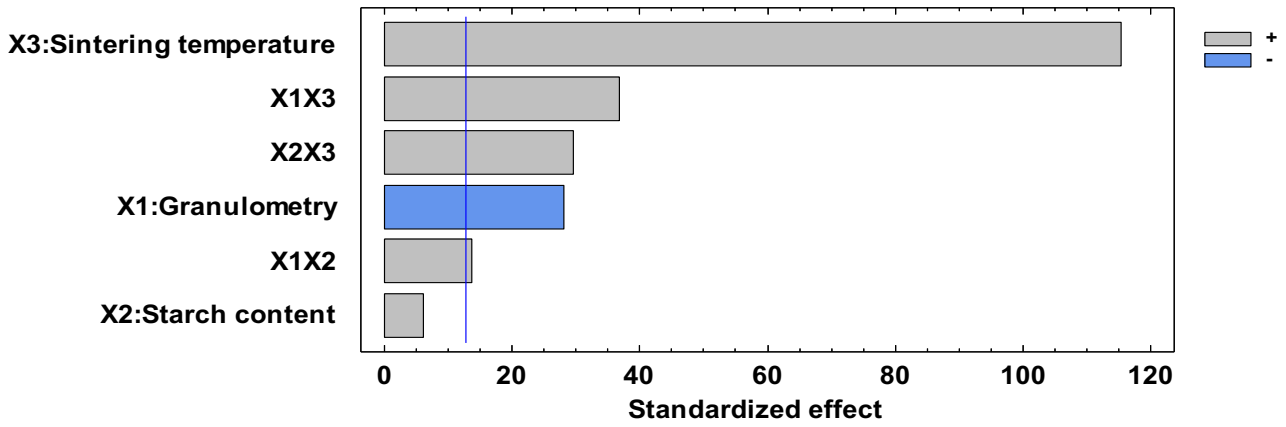


Figure 3: Pareto chart for porosity.

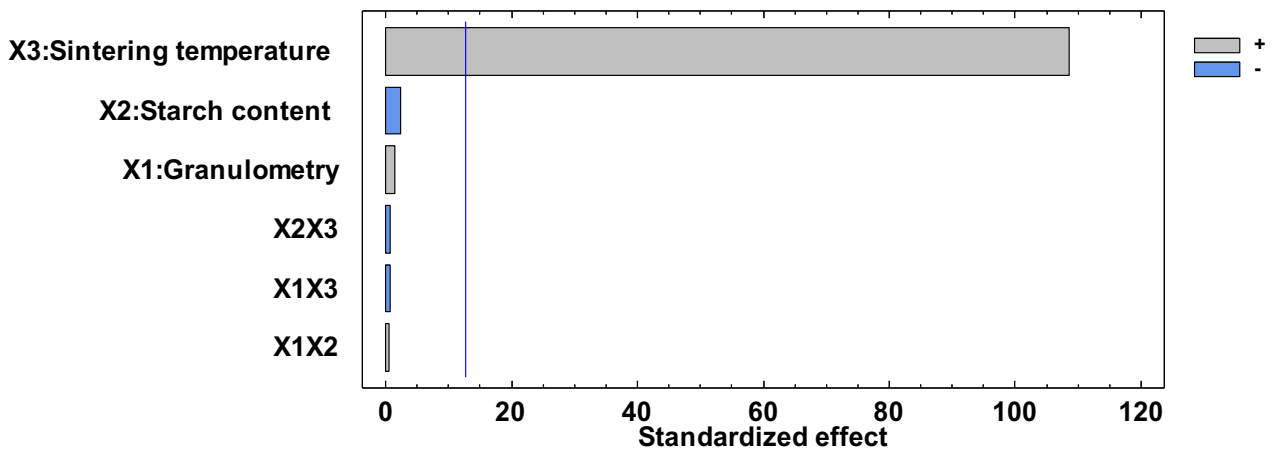


Figure 4: Pareto chart for mechanical resistance.

All factors except starch content influence the porosity as shown in figures 5 and 6. This phenomenon is obviously seen in pareto diagram. Fig. 5 shows that the more the particle size of the increasing powder the more the porosity decreases. On the other hand, the increase in the sintering temperature leads to an increase in percentage of porosity. Sintering corresponds to the thermal consolidation of a material without fusion of at least one of its constituents. It is one of the most delicate and often the most expensive operations in the preparation of ceramics.

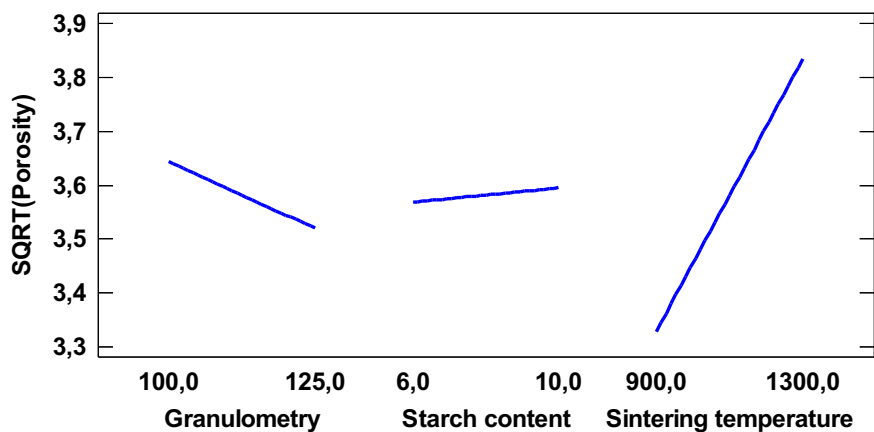


Figure 5: direct effects graph for porosity.

During the thermal cycle, the microstructure is put in place, by material transport between grains, in order to minimize excess interface energies, which is generally accompanied by a decrease in porosity. The latter manifests itself macroscopically by a withdrawal from the "raw" part. We notice very well that the porosity is almost stable when working with 6% or 10% of starch as a porosity agent.

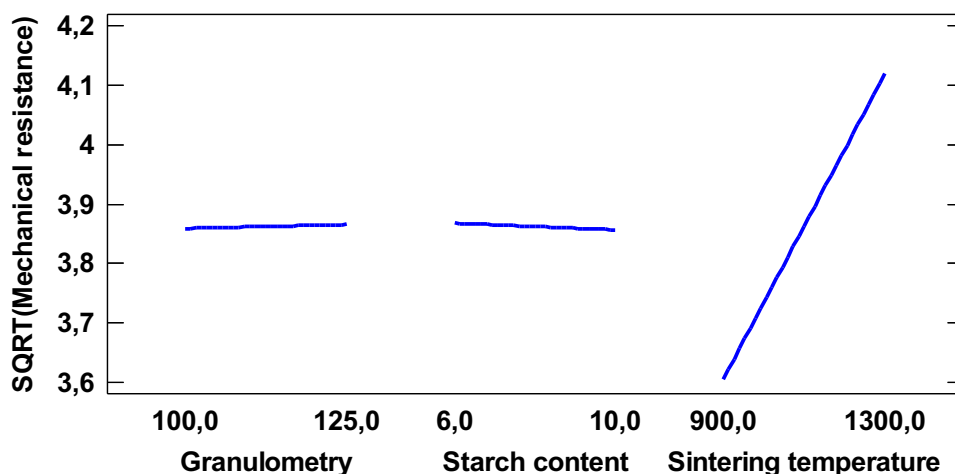


Figure 6: direct effects graph for mechanical resistance.

Table 3 breaks down the variability of porosity into separate lines for each of the effects. It then tests the statistical significance of each of the effects by comparing the root mean with an estimate of the experimental error. In this case, four effects have probabilities less than 0.05, which indicates that they are significantly different from zero at the 95.0% confidence level. The R-squared statistic indicates that the fitted model explains 99,9844% of the variability of porosity. The adjusted R-squared statistic, which is preferable for comparing models with different numbers of explanatory variables, is 99,8905%. The standard error of estimate indicates that the standard deviation of the residuals is 0,0707107. The mean absolute error (AEM) of 0,025 is the mean value of the residuals.

Table 3: Analysis of variance for Porosity

Source	Sum of Square	Degree of freedom	Mean Square	F-Ratio	P-Value
X₁:Granulometry	1.28	1	1.28	256.00	0.0397
X₂:Starch content	0.125	1	0.125	25.00	0.1257
X₃:Sintering temperature	25.92	1	25.92	5184.00	0.0088
X₁X₂	0.405	1	0.405	81.00	0.0704
X₁X₃	2.42	1	2.42	484.00	0.0289
X₂X₃	1.805	1	1.805	361.00	0.0335
total error	0.005	1	0.005		
Total (corr.)	31.96	7			

3.3 Equation model

Interpretation starts with the calculation of the coefficients of the model. The coefficients of the model are represented in **Table 4** below. The statistical analyses showed that the values of the answers would adapt to a model:

$$\text{Porosity (\%)} = 51,6125 - 0,3446X_1 - 0,02525X_3 + 0,00022X_1X_3 + 0,0011875X_2X_3$$

3.4 Response surface

The correlation matrix (table 5) indicates the levels of confusion between the effects. A perfectly orthogonal plane gives a matrix with one on the diagonal and zero everywhere else. All non-zero terms except those in the diagonal indicate that the effect estimates associated with these rows and columns will be correlated. In this case, there is no correlation between the effects. This indicates that we get good estimates of all of these effects

Table 4: Regression coefficients for Porosity.

Coefficient	Estimate
Constant	51.6125
X ₁ :Granulometry	-0.346
X ₂ :Starch content	-2.25625
X ₃ :Sintering temperature	-0.02525
X ₁ X ₂	0.009
X ₁ X ₃	0.00022
X ₂ X ₃	0.0011875

Table 5: Correlation matrix of estimated effects

		(1)	(2)	(3)	(4)	(5)	(6)	(7)
(1)	Average	1	0	0	0	0	0	0
(2)	X ₁ :Granulometry	0	1	0	0	0	0	0
(3)	X ₂ :Starch content	0	0	1	0	0	0	0
(4)	X ₃ :Sintering temperature	0	0	0	1	0	0	0
(5)	X ₁ X ₂	0	0	0	0	1	0	0
(6)	X ₁ X ₃	0	0	0	0	0	1	0
(7)	X ₂ X ₃	0	0	0	0	0	0	1

The graph of response surface in Fig. 7, built after determining the most influential factors, makes it possible to define all the combinations of operating conditions that make it possible to obtain the target value of the response. They are therefore very practical to delineate a desirable or optimal work area.

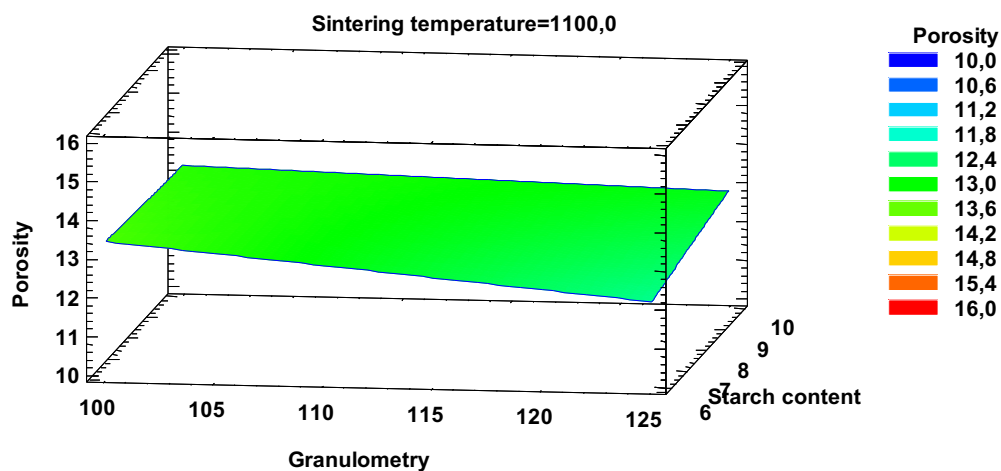


Figure 7: Response surface at sintering temperature 1100°C.

The surface at sintering temperature 1100°C shows that the porosity value varies from 12.4% to 13% for all levels of granulometry and starch content, which confirms the results of the contour of the response surface at the same temperature (fig.8).

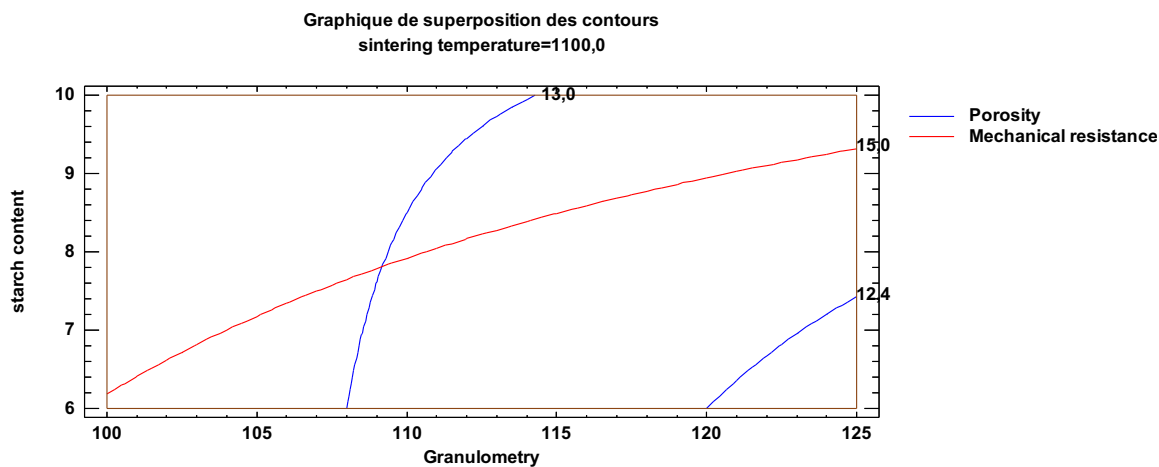


Figure 8: contour of the response surface at sintering temperature 1100°C.

3.5 Optimal response

Our final objective is to maximize the porosity according to the parameters studied. Table 6 and fig.9 show that the theoretical values of the parameters are in the range of experimental values and the theoretical optimum corresponds to the experimental optimum which is equal to 15.6813 %.

Table 6: Factor settings at optimum.

Factor	settings
Granulometry (μm)	125.0
Starch content (%)	10.0
Sintering temperature ($^{\circ}\text{C}$)	1300.0

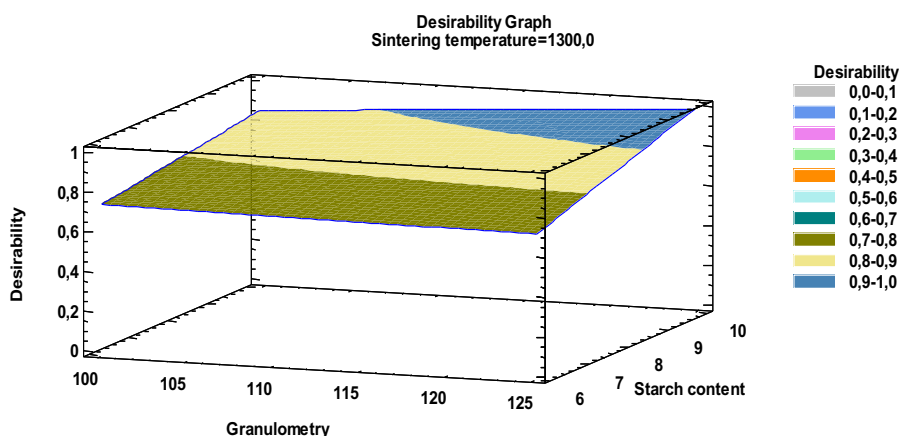


Figure 9: Desirability Graph.

The sintering temperature is an important parameter which controls the pore diameter of the support and its mechanical resistant. The thermal expansion depends also on the firing treatment. Therefore, the best properties of the final support are achieved by adjusting the conditions for sintering. (Table.7.) shows the Pores volume is function of temperature.

Table 7: Pore diameter and pores volume versus firing temperature of the support

Temperature °C	Pore Diameter (Dp:µm)
900	Dp <1µm: 80% <120µm: 20%
1300	Dp <1µm: 70% 300 < Dp < 10: 30%

Conclusion

The use of experimental design is an effective tool to evaluate the important significant factors influencing the elaboration of ceramic membrane. 2 factors namely the Sintering temperature and particle size were found to exert a significant effect on the process. The two factors were optimized using response surface methodology. The best performance of the elaboration of ceramic support membrane was attend at sintering temperature of 1300°C and particle size of 125µm.

the investigation has demonstrated that the sintering temperature is the main controlling factor of the technological properties of ceramic membrane support. The increase of sintering temperature had a positive effect on the mechanical strength and on the porosity due the principal advantage of the organic additives that they are eliminated by combustion during the thermal treatment. The starch content has also a significant influence of the support porosity, this is can be explained that the growth of starch content increases the porosity (Pores former during the burning out) and reduce the mechanical strength.

References

- [1] M. B. Asif and Z. Zhang, “Ceramic membrane technology for water and wastewater treatment: a critical review of performance, full-scale applications, membrane fouling and prospects,” *Chem. Eng. J.*, 418 (2021) 129481, <https://doi.org/10.1016/j.cej.2021.129481>
- [2]. S. Ruthusree, S. Sundarrajan, and S. Ramakrishna, “Progress and perspectives on ceramic membranes for solvent recovery,” *Membranes (Basel)*, 9(10) (2019) 128 <https://doi.org/10.3390/membranes9100128>
- [3] P. Kamgang-Syapnjeu, D. Njoya, E. Kamseu, L. Cornette de saint Cyr, A. Marcano-Zerpa, S. Balme, M. Bechelany and L. Soussan, “Elaboration of a new ceramic membrane support from Cameroonian clays, coconut husks and eggshells: Application for Escherichia coli bacteria retention,” *Appl. Clay Sci.*, 198 (2020) 105836, <https://doi.org/10.1016/j.clay.2020.105836>
- [4] B. Hatimi, J. Mouldar, A. Loudiki, H. Hafidi, M. Joudi, E.M. Daoudi, H. Nasrellah, I.T Lançar, M.A. El mhmmedi, M. Bakasse, “Low cost pyrrhotite ash/clay-based inorganic membrane for industrial wastewaters treatment,” *J. Environ. Chem. Eng.*, 8 (2020) 103646, <https://doi.org/10.1016/j.jece.2019.103646>
- [5] A. Belgada, B. Achiou, S.A. Younssi, F.Z. Charik, M. Ouammou, J.A. Cody, R. Benhida and K. Khaless, “Low-cost ceramic microfiltration membrane made from natural phosphate for pretreatment of raw seawater for desalination,” *J. Eur. Ceram. Soc.*, 41 (2021) 1613–1621, <https://doi.org/10.1016/j.jeurceramsoc.2020.09.064>
- [6] N. Saffaj, N. El baraka, R. Mamouni, H. Zgou, A. Laknifli, S.A. Younssi, Y. Darmane, M. Aboulkacem and O. Mokhtari “New bio ceramic support membrane from animal bone,” *J. Microbiol. Biotechnol. Res.*, 3 (2013) 1–6, www.scholarsresearchlibrary.com

- [7] D. C. Montgomery, *Design and Analysis of Experiments Ninth Edition*. 2017. https://dlwqtxts1xzle7.cloudfront.net/63006338/Douglas_C._Montgomery_Design_and_Analysis_of_Experiments-Wiley_201720200418-93764
- [8] N. El Baraka, M. Addich, A. Fatni, A. Laknifli, N. Saffaj, and M. Ait Baih, “Application of an Experimental Design for Optimizing the Conditions of Ceramic Membranes Elaboration,” *J. Environ. Sci. Pollut. Res.*, 6 (2020) 417–419, <https://doi.org/10.30799/jespr.189.20060103>
- [9] S. T. Narendran, S. N. Meyyanathan, and V. V. S. R. Karri, “Experimental design in pesticide extraction methods: A review,” *Food Chem.*, 289 (2019) 384–395, <https://doi.org/10.1016/j.foodchem.2019.03.045>
- [10] S. J. S. Chelladurai, K. Murugan, A. P. Ray, M. Upadhyaya, V. Narasimharaj, and S. Gnanasekaran, “Optimization of process parameters using response surface methodology: A review,” *Mater. Today Proc.*, 37 (2020) 1301–1304, <https://doi.org/10.1016/j.matpr.2020.06.466>
- [11] M. Sèbe, A. Nassiri, and L. Pendleton, “Using choice experiment designs to evaluate mitigation solutions to reduce whale-ship collisions,” *Mar. Policy*, 124 (2021) 104368. <https://doi.org/10.1016/j.marpol.2020.104368>
- [12] A. Manni, B. Achiou, A. Karim, A. Harrati, C. Sadik, M. Ouammou, S. Alami younssi and A. El Bouari “New low-cost ceramic microfiltration membrane made from natural magnesite for industrial wastewater treatment,” *J. Environ. Chem. Eng.*, 8 (2020) 103906, <https://doi.org/10.1016/j.jece.2020.103906>
- [13] C. Voigt, J. Hubáľková, H. Giesche, and C. G. Aneziris, “Intrusion and extrusion mercury porosimetry measurements at Al₂O₃–C - Influence of measuring parameter,” *Microporous Mesoporous Mater.*, 299 (2020) 110125. <https://doi.org/10.1016/j.micromeso.2020.110125>
- [14] Q. Zeng, S. Chen, P. Yang, Y. Peng, J. Wang, C. Zhou, Z. Wang and D. Yan, “Reassessment of mercury intrusion porosimetry for characterizing the pore structure of cement-based porous materials by monitoring the mercury entrapments with X-ray computed tomography,” *Cem. Concr. Compos.*, 113 (2020) 103726, <https://doi.org/10.1016/j.cemconcomp.2020.103726>
- [15] M. B. Tanis-Kanbur, R. I. Peinador, J. I. Calvo, A. Hernández, and J. W. Chew, “Porosimetric membrane characterization techniques: A review,” *J. Memb. Sci.*, 619 (2021) 118750. <https://doi.org/10.1016/j.memsci.2020.118750>
- [16] R. M. R, V. R, and R. S, “Experimental analysis on density, micro-hardness, surface roughness and processing time of Acrylonitrile Butadiene Styrene (ABS) through Fused Deposition Modeling (FDM) using Box Behnken Design (BBD),” *Mater. Today Commun.*, 27 (2021) 102353. <https://doi.org/10.1016/j.mtcomm.2021.102353>
- [17] C. A. Yanu, J. M. Sieliechi, and M. B. Ngassoum, “Optimization of Ceramic Paste Viscosity Use for the Elaboration of Tubular Membrane Support by Extrusion and Its Application,” *J. Mater. Sci. Chem. Eng.*, 08 (2020) 1–22, <https://doi.org/10.4236/msce.2020.83001>

(2022); <http://www.jmaterenvironsci.com>